

# Stochastic Analysis of THz Band Satellite Channels' Quality

Joonas Kokkonen

Centre for Wireless Communications (CWC), University of Oulu, 90014 Oulu, Finland

Email: joonas.kokkonen@oulu.fi

**Abstract**—The satellite networks are among the most promising platform to achieve true global connectivity. The millimeter wave and THz frequencies on the other hand provide large data rates needed particularly in backhaul and fronthaul networks. This paper looks into the stochastic performance of +100 GHz channels in satellite uplink and downlink cases. It is shown that while SNRs can be quite good, there are still great challenges to go around very large losses and the large outage probabilities that those cause. This is particularly the case when we add on the channel losses possible rain and cloud losses, antenna misalignment losses, or any other losses that can occur in the satellite channels.

## I. INTRODUCTION

One of the greatest challenges of future networks is to bring the internet to all and make it accessible to everyone [1]. Satellite networks are the obvious choice to achieve global coverage and they are the only choice in many cases as there are vast areas around the world that are difficult or impossible to cover by terrestrial networks. The millimeter wave (mmWave, 30–300 GHz) and THz band (>300 GHz) are seen as very promising platforms for the applications that need very high data rates [2], [3]. Although, technical challenges with these frequencies have pushed them off the first generation of 6G systems, the high frequencies are still in the horizon in various applications. Controversially to their usually short link distances, satellite networks are seen as one potential application for high mmWave communications (100–300 GHz) [4], [5].

THz band satellite systems have been studied in quite a number of recent works [4]–[13]. These works have shown that high frequency ultra long links are indeed possible. This is especially the case with the high atmosphere applications, such as airplane to satellite links, because the atmospheric losses therein are much smaller than on terrestrial communications. In general, the non-terrestrial networks (NTNs) have become active research field due to vast potential of the satellite-based systems. Some downsides are large propagation distances that also cause larger latencies. When talking about the high mmWave frequencies, the biggest challenge is to provide large enough antenna gains to overcome the large channel losses. Starlink and various airplane internet providers have shown that mmWave has a great future in global internet coverage.

This paper focuses on stochastic analysis of +100 GHz satellite downlink and uplink applications. The main focus is on analysing airplane to satellite links in the case of antenna limitations and multiple serving satellites. There are some

works on stochastic modeling of the satellite links, such as [14]–[16]. The closest to this paper is our previous paper on the topic [5] where we derived the most of the models used in this paper. It will be shown that the achievable SNRs are very good if large aperture antennas are used. Antenna non-idealities, e.g., limited field of view being one, can hinder the performance of the system quite a bit. Furthermore, outage probabilities can be very high even with sufficiently high SNRs due to great variance in the signal levels. This suggests a need for good amount of channel coding in all situations with limitations on the usable modulation methods. Still, the high-frequency satellite systems seem very promising, but many of the system choices such as antennas will have an impact on the overall system design and required densities of the satellites to make the high frequency satellite systems viable and reliable option to slower but more robust low frequency systems.

The rest of this paper has been organized as follows. The system model, system geometry, and stochastic models are given in Sec. II, the numerical results are given in Sec. III, and conclusions are given in Sec. IV.

## II. SYSTEM AND LINK MODELS

In this section, we go through the system model and its geometry. Then we will give the stochastic propagation models that allow calculation of the average signal power in various satellite scenarios, such as satellite to airplane case or satellite to Earth case. The utilized system model and the stochastic models were given in our previous work in [5]. This work mainly extends the analysis and adds a consideration of a situations where the antenna beams cannot be directed to see the entire horizon, but are limited in elevation angles. Therefore, the general system model is presented here as there are small changes to the model presented in [5] in order to limit the visibility of the antennas.

### A. System Model and Geometry

The system is illustrated in Fig. 1. We base the system model on imaginary spherical caps that surround a user. For instance, if a user (e.g., an airplane) at altitude  $h_a$  can beamform to all directions in its horizon, all the visible satellites are on a spherical cap suspended by the altitude of the user and the orbit height  $h_s$  of the satellites. This spherical cap has an area

$$A_{sp} = 2\pi(R + h_a)^2(1 - \cos(\theta)), \quad (1)$$

where  $R$  is the radius of Earth and  $\theta$  is the angle suspended between the edge of the spherical cap and the core of Earth. This angle can be given as

$$\theta = \cos^{-1} \left( \frac{R + h_a}{R + h_s} \right). \quad (2)$$

If we would imagine that the user cannot see from horizon to horizon, but the visibility is limited to some maximum angle  $\beta$  about the zenith (as seen in Fig. 1), then the user would see a spherical cap that would have an area

$$A'_{\text{sp}} = 2\pi(R + h'_a)^2(1 - \cos(\theta')), \quad (3)$$

where

$$h'_a = h_a + r_{\min} \cos(\beta), \quad (4)$$

and

$$\theta' = \cos^{-1} \left( \frac{R + h'_a}{R + h_s} \right), \quad (5)$$

where  $r_{\min} = h_s - h_a$  is the minimum distance between the satellite and the user. Then stochastically, a network of same density of satellites is thinned by a factor  $A'_{\text{sp}}/A_{\text{sp}}$ . The impact of this thinning is shown via stochastic geometry in the numerical results. In order to calculate the other losses, such as free space path loss, we also need the distance from the user to satellite, as well as the atmospheric structure in order to calculate the atmospheric losses (molecular absorption loss). The details are given in [5]. Distance from the satellite to airplane is given by

$$r_{as}(\theta) = \sqrt{(R + h_a)^2 + (R + h_s)^2 - 2(R + h_a)(R + h_s) \cos(\theta)}, \quad (6)$$

and the path through the atmosphere is given by

$$r_{\text{atm}}(\theta, x) = (R + h_a) \cos(\epsilon) + \frac{1}{2} \sqrt{(-2(R + h_a) \cos(\epsilon))^2 - 4((R + h_a)^2 - (R + x)^2)}, \quad (7)$$

where  $x$  is the vertical path through the atmosphere, and  $\epsilon$  is the angle between Earth's core and satellite looked from the airplane

$$\epsilon = 180^\circ - \alpha - \theta, \quad (8)$$

where  $\alpha$  is the angle between the satellite and the airplane looked from the satellite

$$\alpha = \sin^{-1} \left( \frac{(R + h_a) \sin(\theta)}{r_{as}(\theta)} \right). \quad (9)$$

The latter terms will have to be adjusted with  $\theta'$  and  $h'_a$  if the user has limited beamforming. This could be, for instance because of mechanical limitations of the antenna system, or just limitation to the antenna radiation pattern.

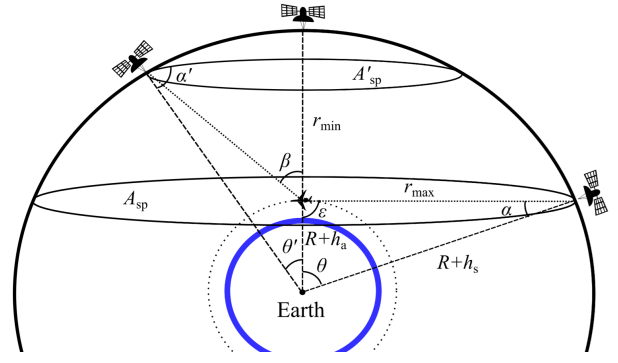


Fig. 1. System model and geometry utilized in this paper.

## B. Static link loss

The signal power at the receiver can be given similarly as in [4], [5]

$$S(f, r_{as}(\theta)) = \frac{c^2 P_{\text{Tx}} G_{\text{Tx}} G_{\text{Rx}}}{(4\pi r_{as}(\theta) f)^2} e^{-\int_{h_a}^{h_l} \kappa_a(f, r_{\text{atm}}(\theta, x)) dx}, \quad (10)$$

where  $P_{\text{Tx}}$  is the transmit power,  $G_{\text{Tx}}$  and  $G_{\text{Rx}}$  are the Tx and Rx antenna gains,  $f$  is the frequency,  $c$  is the speed of light,  $h_l$  is the upper limit of the atmosphere, which we assume to be above the satellite orbits in this work causing this limit to be the satellite orbit altitude, and  $\kappa_a(f, r)$  is the absorption coefficient. The absorption coefficient in satellite systems is given, e.g., in our previous work in [4] including the atmospheric composition. It can also be calculated, e.g., via ITU-R models [17]. Other losses are assumed to be negligible, although those are shortly discussed in the numerical results and would be easy to add in the above equation if wanted. Lastly, we assume parabolic antennas due to their large gain at high frequencies. The gain of those is given by

$$G(f) = A_e \left( \frac{\pi d_A}{\lambda} \right)^2, \quad (11)$$

where  $A_e$  is the aperture efficiency,  $d_A$  is the diameter of the reflector, and  $\lambda$  is the wavelength. The parabolic antennas will require mechanical beamsteering and most likely multiple antennas to connect and search for the next satellite simultaneously.

## C. Stochastic received power

Given the above geometry, we can give the stochastic path loss and received power, respectively, as [5]

$$\text{PL}_{\text{ave}}(f) = \frac{(1 - \cos(\theta))(4\pi f)^2}{c^2} \times \left( \int_0^\theta \frac{\sin(\phi)}{r_{as}^2(\phi)} \exp \left( - \int_{h_a}^{h_l} \kappa_a(f, r_{\text{atm}}(\phi, x)) dx \right) d\phi \right)^{-1}, \quad (12)$$

TABLE I  
THE SIMULATION PARAMETERS

Parameter	Value
Total transmit power	1 W
Bandwidth	1 GHz
Rx noise figure	7 dB
Rx temperature	300 K
Sat. antenna diam.	1 m
User antenna diam.	0.5 m

and

$$S_{\text{ave}}(f) = \frac{c^2 N P_{\text{Tx}} G_{\text{Tx}} G_{\text{Rx}}}{(1 - \cos(\theta))(4\pi f)^2} \times \int_0^\theta \frac{\sin(\phi)}{r_{\text{as}}^2(\phi)} \exp\left(-\int_{h_a}^{h_t} \kappa_a(f, r_{\text{atm}}(\phi, x)) dx\right) d\phi, \quad (13)$$

where  $N$  is the number of serving satellites at any given time. We will look into the impact of the number of serving satellites in the numerical results, although, their impact in stochastic sense is quite straightforward. In reality, multiple serving satellites would require multiple antenna systems at the user location, since at high frequencies the beamforming is mostly done via mechanical antennas. However, on lower mmWave bands antenna arrays are even commercially used option (e.g., Starlink).

### III. NUMERICAL RESULTS

The stochastic performance of +100 GHz satellite systems via the above presented tools is done by applying parameters given in Table I. These are assumed in all the results unless otherwise stated.

Let us begin by first looking into the average SNR obtained by

$$\text{SNR} = \frac{S_{\text{ave}}(f)}{N_0}, \quad (14)$$

where  $N_0 = k_B T W N_f$ , where  $k_B$  is the Boltzmann constant,  $T$  is the receiver temperature,  $W$  is the system bandwidth, and  $N_f$  is the system noise figure. Figs. 2 and 3 show the average SNRs for various antenna diameters at Tx and Rx. We can see that the much lower absorption loss at high atmosphere user (Fig. 2) omits quite a lot of the channels losses compared to users on Earth (Fig. 3). In fact, on Earth, the most of the frequencies above 150 GHz are hard to reach due to large losses in the atmosphere. In contrast, the high altitude system gain SNR when moving to higher frequencies. This effect is shown in many results here and it is caused by the fixed aperture antennas that generate the more gain the higher is the frequency. In reality, the ability of the RF electronics to generate power as a function of frequency would not make it possible to utilize this gain fully, but the antennas do theoretically generate more gain as a function of frequency if the aperture is kept fixed.

Looking into limiting the antenna visibility angle in Figs. 4 and 5 it is straightforward to understand that limiting the

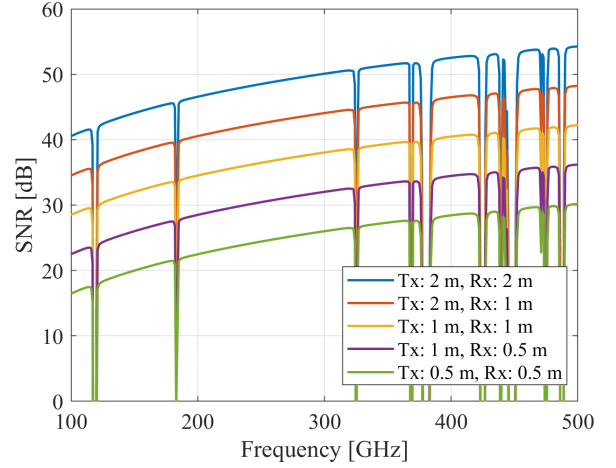


Fig. 2. Average SNR of airplane-satellite link with 10 km airplane altitude with different antenna diameters at the Rx and Tx as a function of frequency.

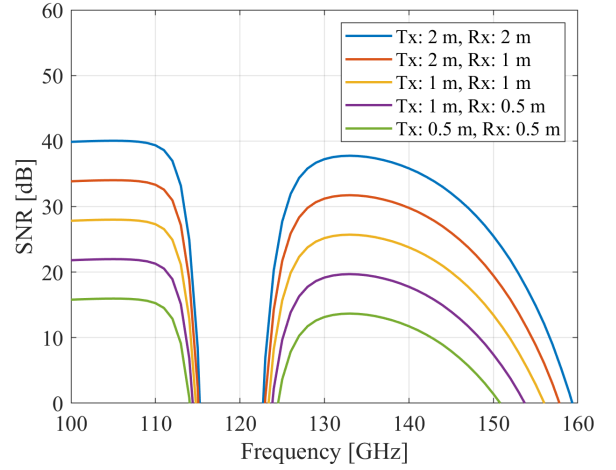


Fig. 3. Average SNR of ground-satellite link with different antenna diameters at the Rx and Tx as a function of frequency.

potential points of contact in the sky will in average degrade the signal levels. This kind of limitations could be caused by physical limitations of the antenna system or the beam patterns of the antennas. Although it does not directly decrease the signal levels if there are serving satellites within the field of view of the antenna(s), this kind of limitation may cause some implications on the overall system design and network density requirements to make sure there is always a satellite available. This becomes a bigger issue at higher frequencies due to the need for ever higher gains when moving to higher and higher in spectrum.

Finally, let us look into the outage shown in Figs. 6–8 for QPSK, 16-QAM, and 64-QAM modulations, respectively. The results herein were obtained by using 0.5 meter antenna at both airplane at 10 km altitude and at satellite. The modulations set the threshold for the outage probability

$$P_o = 1 - P_s = \mathcal{P}(S(f) > \delta N_0), \quad (15)$$

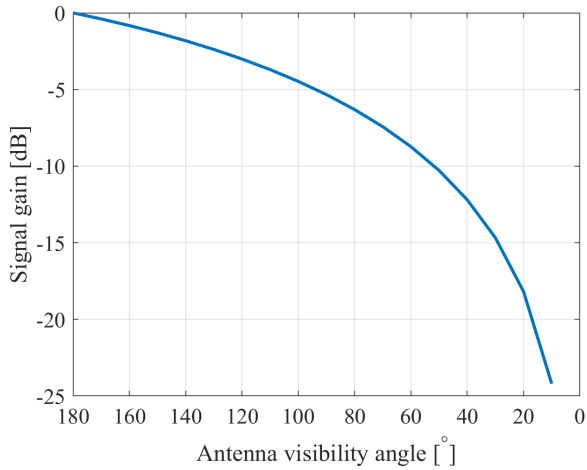


Fig. 4. Average degradation of signal level when limiting the users antenna visibility angle given a fixed satellite network density.

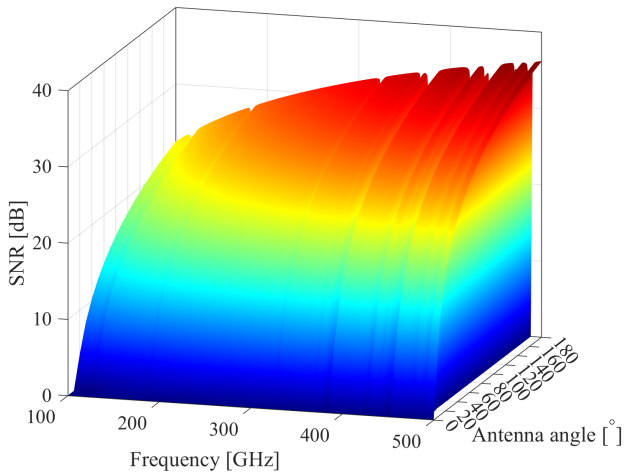


Fig. 5. Average SNR degradation when limiting the users antenna visibility angle given a fixed satellite network density as a function of frequency at an airplane at 10 km altitude.

where  $P_o$  is the outage probability,  $P_s$  is the success probability, and  $\delta$  is the set threshold. In the other words, the threshold set the boundary for the expected SNR ( $S(f)/N_0$ ). The QAM SNR limits were estimated by assuming rectangular gray coded QAM modulation that have the SNR limit based on the target bit error probability (BER)

$$\text{SNR}_{\text{QAM}} = \frac{(M-1)}{3 \log_2(M)} \left[ Q^{-1} \left( \frac{\log_2(M) \cdot \text{BER}}{4 \left(1 - \frac{1}{\sqrt{M}}\right)} \right) \right]^2, \quad (16)$$

where  $M$  is the modulation order. These yield SNR limits given in Table II for target BER of  $10^{-6}$ . The outage probability does not have closed form expression and hence the outages in 6–8 were studied with a simulation model by using the geometry and loss models presented in the previous section. We can see that the outage probabilities are rather

TABLE II  
SNR THRESHOLDS FOR QAM MODULATIONS WITH TARGET BER  $10^{-6}$

Modulation	SNR limit
QPSK SNR limit	10.5 dB
16-QAM SNR limit	14.4 dB
64-Qam SNR limit	18.8 dB

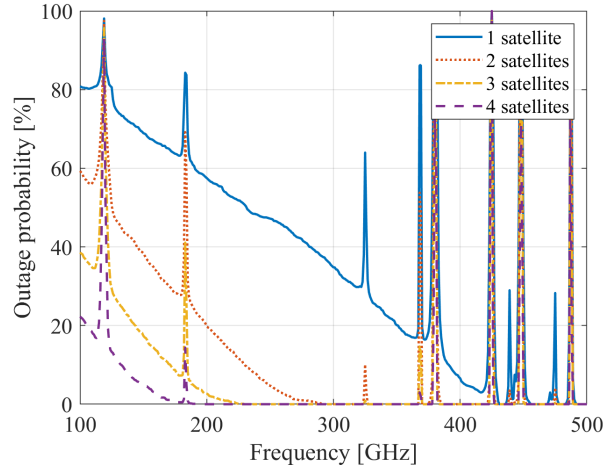


Fig. 6. The outage probability of airplane to satellite link using QPSK with different numbers of serving satellites.

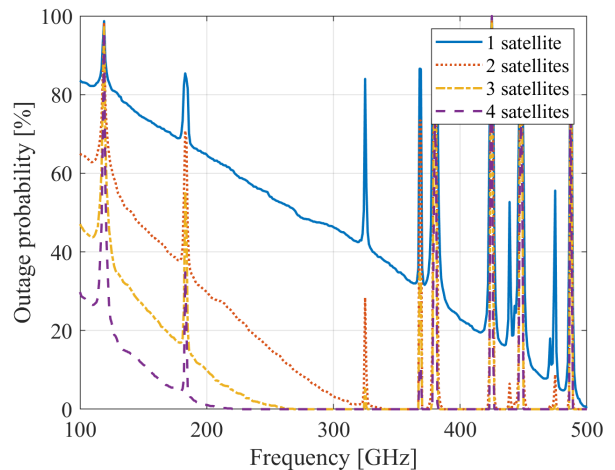


Fig. 7. The outage probability of airplane to satellite link using 16-QAM with different numbers of serving satellites.

high even if the average SNRs are quite good. This means that we are on the edge of the SNR and we preferably would like employ as large antennas as possible to stay at acceptable SNR limits. There are a couple of notes to be made of these results. Firstly, we do not consider any channel coding. A real system would be more tolerant to errors via coding. Secondly, throughout the results we assume clear sky. Rain and clouds can bring anything from 0 to +20 dBs of extra losses [18], [19]. Also, antenna misalignment losses may bring significant losses on top of the considered ideal system [20]. This means

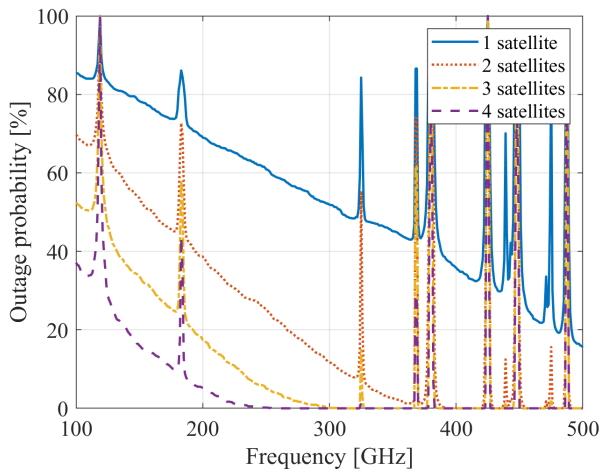


Fig. 8. The outage probability of airplane to satellite link using 64-QAM with different numbers of serving satellites.

that there is a lot of analysis still ahead when considering very high frequencies for satellite applications. In one hand, they can create opportunities in providing true global backhaul network connecting all the people to high speed internet, but using the high frequencies will have severe limitations of some are fundamentally unachievable by technological development. Still, the future of the high frequencies look very promising also in the satellite domain.

#### IV. CONCLUSIONS

The high frequency satellite systems were analysed in this paper. It was shown that they are quite vulnerable to many losses even if on average good signal levels can be achieved if large antenna gains can be provided. All in all, +100 GHz satellite systems seem a promising way to connect the world to high speed backhaul network, but there are strict limitations on these systems. With huge distances come huge problems. On a good day the link can work perfectly, but stormy day (at above 100 GHz) can mean loss of the signal completely. There are great challenges ahead to understand all the limitations and to find solutions how to overcome some problems that physically can be solved to make the high frequency satellite networks reality in the future.

#### ACKNOWLEDGMENT

This work was supported by the Research Council of Finland project TERASAT under grant no. 357711. This research was also supported by the Research Council of Finland 6G Flagship Programme under grant no. 346208.

#### REFERENCES

[1] H. Saarnisaari, S. Dixit, M.-S. Alouini, A. Chaoub, M. Giordani, A. Kliks, M. Matinmikko-Blue, and N. Zhang, Eds., *6G White Paper on Connectivity For Remote Areas*, ser. 6G Research Visions, 6G Flagship, University of Oulu, 2020, no. 5. [Online]. Available: <http://urn.fi/urn:isbn:9789526226750>

[2] I. F. Akyildiz, J. M. Jornet, and C. Han, "Terahertz band: Next frontier for wireless communications," *Elsevier Phys. Commun.*, vol. 12, pp. 16–32, Sep. 2014.

[3] M. Latva-Aho and K. Leppänen, Eds., *Key drivers and research challenges for 6G ubiquitous wireless intelligence*, ser. 6G research visions, University of Oulu, Sep. 2019, no. 1.

[4] J. Kokkonen, J. M. Jornet, V. Petrov, Y. Koucheryavy, and M. Juntti, "Channel modeling and performance analysis of airplane-satellite terahertz band communications," *IEEE Transactions on Vehicular Technology*, vol. 70, no. 3, pp. 2047–2061, 2021.

[5] J. Kokkonen, J. M. Jornet, and M. Juntti, "Stochastic geometry framework for thz satellite-airplane network analysis," in *2021 IEEE International Symposium on Dynamic Spectrum Access Networks (DySPAN)*, 2021, pp. 67–72.

[6] J. Y. Suen, M. T. Fang, S. P. Denny, and P. M. Lubin, "Modeling of terabit geostationary terahertz satellite links from globally dry locations," *IEEE Transactions on Terahertz Science and Technology*, vol. 5, no. 2, pp. 299–313, 2015.

[7] M. Saqlain, M. N. Idrees, S. Wang, and X. Yu, "Channel modeling and performance analysis of fixed terahertz Earth-satellite links in the low- and mid-latitude regions," *Optical Engineering*, vol. 60, no. 3, pp. 1–16, 2021. [Online]. Available: <https://doi.org/10.1117/1.OE.60.3.036103>

[8] M. Civas and O. B. Akan, "Terahertz wireless communications in space," *arXiv*, pp. 1–7, 2021. [Online]. Available: <https://arxiv.org/abs/2110.00781>

[9] M. Saqlain, N. M. Idrees, X. Cao, X. Gao, and X. Yu, "Feasibility analysis of opto-electronic thz earth-satellite links in the low- and mid-latitude regions," *Appl. Opt.*, vol. 58, no. 25, pp. 6762–6769, Sep 2019. [Online]. Available: <http://www.osapublishing.org/ao/abstract.cfm?URI=ao-58-25-6762>

[10] S. Nie and I. F. Akyildiz, "Channel modeling and analysis of inter-small-satellite links in terahertz band space networks," *IEEE Transactions on Communications*, pp. 1–1, 2021.

[11] L. Bai, Z. Zhu, and X. Li, "Analysis of THz space communication link based on STK," *IOPscience Journal of Physics: Conference Series*, vol. 1971, no. 1, p. 012073, jul 2021. [Online]. Available: <https://doi.org/10.1088/1742-6596/1971/1/012073>

[12] S. U. Hwu, K. B. deSilva, and C. T. Jih, "Terahertz (thz) wireless systems for space applications," in *IEEE Sens. Appl. Symp. Proc.*, 2013.

[13] J. Yang, H. Li, and Z. Xu, "Analysis of channel characteristics between satellite and space station in terahertz band based on ray tracing," *Radio Science*, vol. 56, no. 9, p. e2021RS007290, 2021, e2021RS007290 2021RS007290. [Online]. Available: <https://agupubs.onlinelibrary.wiley.com/doi/abs/10.1029/2021RS007290>

[14] N. Okati, T. Riihonen, D. Korpi, I. Angervuori, and R. Wichman, "Downlink coverage and rate analysis of low earth orbit satellite constellations using stochastic geometry," *IEEE Transactions on Communications*, vol. 68, no. 8, pp. 5120–5134, 2020.

[15] D.-H. Jung, J.-G. Ryu, W.-J. Byun, and J. Choi, "Performance analysis of satellite communication system under the shadowed-rician fading: A stochastic geometry approach," *arXiv*, pp. 1–12, Apr. 2021. [Online]. Available: <https://arxiv.org/abs/2104.13010>

[16] A. Talgat, M. A. Kishk, and M.-S. Alouini, "Stochastic geometry-based analysis of leo satellite communication systems," *IEEE Communications Letters*, vol. 25, no. 8, pp. 2458–2462, 2021.

[17] *ITU-R (2009) Recommendation P.676-8, Attenuation by atmospheric gases*, International Telecommunication Union Radiocommunication Sector Std.

[18] *ITU-R (2013) Recommendation P.840-6, Attenuation due to clouds and fog*, International Telecommunication Union Radiocommunication Sector Std.

[19] *ITU-R (2005) Recommendation P.838-3, Specific attenuation model for rain for use in prediction methods*, International Telecommunication Union Radiocommunication Sector Std.

[20] J. Kokkonen, A.-A. A. Boulogeorgos, M. Aminu, J. Lehtomäki, A. Alexiou, and M. Juntti, "Impact of beam misalignment on THz wireless systems," *Elsevier Nano Communication Networks*, vol. 24, pp. 1–9, May 2020.